JOURNAL OF APPLIED ELECTROCHEMISTRY 19 (1989) 10–18

Stibine and arsine generation from a lead–acid cell during charging modes under a utility load-leveling duty cycle

R. VARMA, Z. TOMCZUK, S. KAZADI, N. P. YAO

Chemical Technology Division, Argonne National Laboratory, 9700 South Cass Avenue, Argonne, IL 60439, USA

Received 25 May 1988

An investigation has been conducted to determine the generation of stibine and arsine during charging of a large industrial lead–acid cell (2250 Ah capacity at 5-h rate) under contemplated utility load-leveling duty cycles. The toxic gases generated were absorbed in a 3 N H_2SO_4 solution containing KI and I_2. The antimony and arsenic contents of the absorber solutions were determined by colorimetry and atomic absorption spectrophotometry, respectively. Total emissions of stibine and arsine, as well as their generation-rate profiles, were determined each week in experiments consisting of four charges and one equalization charge/cycles. In addition, hydride generation during successive, daily equalization charges was monitored. The average emissions of stibine and arsine from the lead–acid cell during a charge cycle, which consisted of charging the cell (discharged to 80% of its rated capacity) at constant 290 A for 5–6 h to 2.45 V followed by taper charge at the same voltage for 3 h, were observed to be 10.1 $\pm$ 1.4 mg of SbH_3 and 0.33 $\pm$ 0.06 mg of AsH_3. The corresponding averages determined for weekly equalization charges conducted at 2.55 V for 4 h were 25.5 $\pm$ 0.7 mg SbH_3 and 0.23 $\pm$ 0.01 mg AsH_3.

1. Introduction

Lead–acid batteries have potential near-term applications in utility load-leveling and electric-vehicle propulsion. The contemplated use of these industrial lead–acid batteries for load-leveling calls for daily storage of off-peak base-load energy through charging and subsequent delivery of stored energy through discharging during periods of high load demand.

State of the art lead–acid battery grids, particularly those used in positive plates, are typically fabricated from lead–antimony alloys containing small amounts of arsenic. The antimony and arsenic contents usually range from 2 to 6% Sb and from 0.1 to 0.2% As. Antimony improves the metallurgical properties of the alloys and makes the fabrication of grids easier. Arsenic is believed to reduce the corrosion of the grid and thereby helps lower the self discharge of the cell. However, a potential disadvantage of the use of these alloys in the lead–acid cell grids is that stibine and arsine are generated during the charging of the battery.

Stibine and arsine are extremely toxic gases; the toxicity of these gases can be compared with that of phosgene. In 1976, the National Institute for Occupational Safety and Health (NIOSH) set limits [1] on occupational exposures to these gases: 0.05 ppmv or 0.2 mg cm^{-3} for AsH_3 and 0.1 ppmv or 0.5 mg m^{-3} for SbH_3, time-weighted averages (TWAs). Cases of poisoning by toxic hydrides generated in lead–acid batteries have been reported. Poisoning of 30 crew members aboard a British submarine was attributed to stibine and arsine, which was generated [2] from lead–acid batteries operating under conditions of poor ventilation. The battery grids were composed of a lead–antimony alloy which contained 12% Sb and 0.2% As.

A number of experimental and theoretical investigations on the electrolytic formation of stibine [3–5] and arsine [3] have been reported in the literature. Stibine and arsine are generated [6–8] at the negative electrode during charging of lead–acid cells. The generation of stibine [6, 7] begins when the cell voltage approaches a value of 2.45 V, attains a maximum value during the initial period of overcharge and then drops to lower levels if overcharge is continued. Furthermore, stibine evolution increases [9] with increased antimony content of the grid alloy. However, there is no quantitative data for generation rates and total production of these gases under load-leveling charging and equalization-charging conditions. Agruf *et al.* [10] have suggested that the kinetics of stibine formation depend on rate of corrosion of positive grids, on the nature of the separator, and most of all on the concentration and form of antimony on the negative electrode surface during battery charging operation. The generation of stibine is preceded by dissolution of antimony into acid electrolyte, transport of antimony species towards the negative and deposition of antimony on the plate; this is supported by studies conducted by Herrman *et al.* [11] and others

0021-891X/89 $03.00 + .12

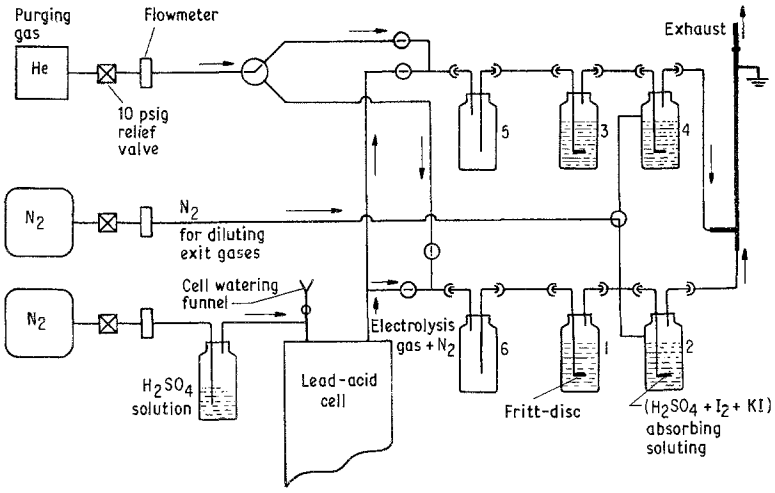

Fig. 1. Schematic of stibine and arsine collection system; 5 and 6 are empty bottles.

[12]. Preliminary reports on stibine and arsine emissions from lead–acid batteries (including prototype electric vehicles) were presented earlier [13].

The purpose of this study was to determine the dependence of hydride emission rates on battery operational parameters such as the cell voltage and charging current.

The experimental work reported below was aimed at quantitative monitoring of SbH_3 and AsH_3 as well as concomitant acquisition of electrical and electrolyte temperature data from an industrial lead–acid cell during charging modes. A schedule of four daily discharge–charge cycles, followed by a weekly equalization charge, was chosen to simulate contemplated utility application.

2. Experimental details

2.1. *Experimental apparatus details*

The experimental apparatus was designed for efficient collection of SbH_3 and AsH_3 in an absorbing solution and for acquisition of cell data such as current, voltage, ampere-hours, watt-hours, ambient temperature and electrolyte temperature during charging of the lead–acid cell.

The system for collecting stibine and arsine consisted of inert Teflon and Fluran fluoroelastomeric tubing, 70-Pa (10 psig) relief valves, gas flowmeters equipped with precision metering valves, Pyrex stopcocks with Teflon screw-in plugs, Pyrex ball/socket joints with Viton O-rings, 3-way valves and Pyrex gas bubblers fitted with gas inlet tubing ending in porous (pore size, 60–70 μm) disc elements for dispersion of the electrolysis gas through the absorbing solution. The schematics of the gas-collection system are illustrated in Fig. 1. Two separate gas-collection trains, capable of being used in an alternate manner (see Fig. 1), allowed continuous sample collection throughout the duration of any charge cycle. Each train contained an empty bottle to prevent accidental back-suction of the absorbing solution into the cell and two gas bubblers, which contained 100 ml of the absorbing solution. The exit gas lines from the two collection trains were connected to a wide-bore copper vent tube (1.30 dia.) leading to the top of a fume hood. The tip of the vent tube was electrically grounded to prevent sparking from static charge build-up. The remaining portion of the system consisted of a computer-controlled Robicon cell cycler, an HP model 1750 two-pen strip chart recorder and a data-processing facility.

The 1000-A cell cycler with continuous rating to 30 V, manufactured by Robicon Company, was interfaced with a computer to maintain a chosen schedule of cell cycling over the entire test period. The Varian Minicomputer (620/16 bit), along with paper tape reader/printer, magnetic tape unit, console and slave teletype (for manual control) were used for control functions. The computer was operated under a locally modified version of Varian's BEST (Basic Executive Scheduler and Timer) unit which contained the cell cycling test schedule. The data acquisition system (VIDAR Corporation), consisting of programmable multimeters with measurement capability for voltage, current, resistance, time and the scanning system were activated under computer control. An HP Model 1750 strip chart recorder and a Fluke digital voltmeter were used for usual monitoring of cell voltage and current in an auxiliary data acquisition capacity.

The 4.2 kWh (2250 Ah at 5-h rate to 1.75 V) lead–acid cell used in this study was an industrial cell (Type C-160-31 manufactured by C & D Batteries) containing 31 grid plates of lead–antimony alloy. The positive grids contained $\sim$4.6% Sb and $\sim$0.08% As, whereas the negative grids contained $\sim$4.3% Sb and $\sim$0.08% As. The active material of the negative plates of this cell was found to contain $\sim$0.15% Sb and $<$0.005% As prior to the experiments described in this report. The separators were made of microporous rubber. The cell had been given about 100 shallow cycles consisting of two 600 Ah discharges, each followed by an equalization charge administered each week during the 52 weeks prior to the cell's arrival at our Laboratory. The upper part of the cell was modified by C & D Batteries as shown in Fig. 2. Inlet and outlet ports in the cell top were provided to permit carrier gas to flow through the space above the moss plate of the cell and thus sweep charging-generated gases out of the cell and into the gas bubblers. A polyethylene tube,

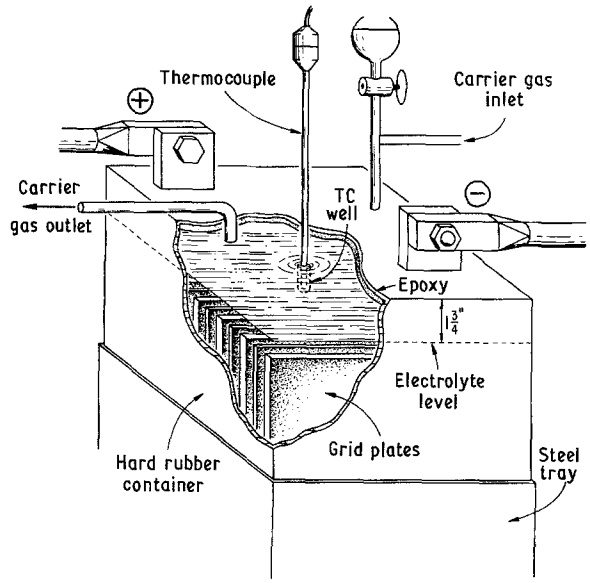

Fig. 2. Modified top of lead–acid cell with ports for temperature measurement and for gas inlet and outlet.

closed at its lower end and immersed about 1.3 cm in the electrolyte through the cell top, accommodated an iron–constantan thermocouple for measuring the electrolyte temperature during cycling.

2.2. *Discharge/charge and equalization charge cycles*

Experiments to simulate the anticipated practice in load-leveling applications involved four consecutive daily discharge and charge cycles of the cell and one weekly equalization charge. The cycling charge schedule for a typical week is shown in Fig. 3. The cell was discharged for 5 h at constant current to 80% of the rated capacity. The discharge cell in each case was charged at constant current (290 A) for 5–6 h to 2.45 V. This was followed by a current-limited, constant-voltage (tapering) charge at 2.45 V for 3 h. The weekly equalization charge consisted of charging the battery at 2.45, 2.55 or 2.65 V for 3–4.5 h.

During another set of experiments, the cell in the fully charged condition was given an equalization charge for 4 h at 2.55 V on 5 successive days and at 2.45 V on 1 day. The cell was maintained on open circuit between the equalization charges.

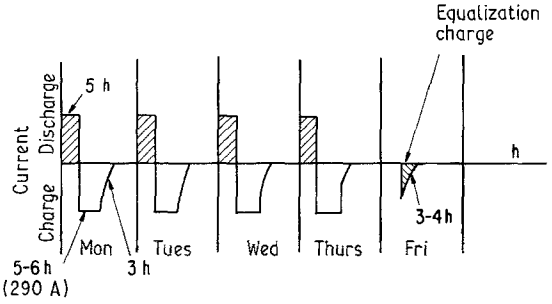

Fig. 3. Weekly discharge/charge schedule.

2.3. *Experimental procedures*

Stibine and arsine are extremely toxic gases; in addition, the mixture of H_2 and O_2 gases generated during the overcharge and equalization charge period may interact explosively. Therefore, to ensure safe operation, nitrogen was used as a carrier gas and was also added to the gas mixture in the second absorbing bottle of each collection train (see Fig. 1) to dilute the resulting gaseous mixture. As an added safety feature, the copper vent tube would prevent flash backs. In addition, calculations indicated that the gaseous material would exit at 10 feet per second through this vent, so as to prevent an explosion.

The electrolysis gas mixture (H_2, O_2, SbH_3, H_2O) was conducted out of the cell by carrier gas flowing at rates ranging up to 1000 ml min^{-1}. The gaseous stream was allowed to bubble through the absorbing solutions (3 N H_2SO_4 containing 8% KI and 1% I_2 by weight) contained in the two trains. When a preselected collection time had elapsed, gas flow was switched to the second train. The absorbing solutions in the bottles of the first train constituted Sample 1; Sample 2 was collected using the second train. Analyses showed that SbH_3 and AsH_3 were completely absorbed by the first absorber in each train when the flow rate of N_2 was < 1500 ml min^{-1} (the second absorber contained no Sb or As). Subsequently, only the first solution in a train was analyzed. The gas lines and the spaces above the absorbing solutions in the bottles were purged (see Fig. 1) for 2–3 min with helium gas to remove any traces of residual toxic gases before transferring the samples into vials for chemical analysis. Typically, 10–15 samples were collected during each charge cycle;

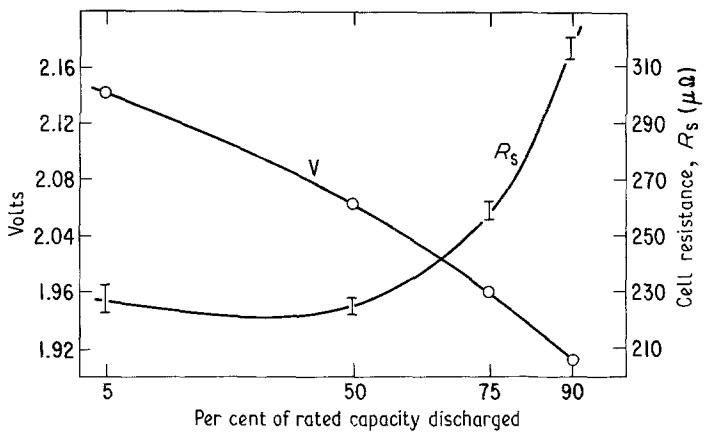

Fig. 4. Variation of internal resistance and all voltage with percent rated capacity discharged.

samples were taken more frequently during initial portions of these cycles. Generation-rate profiles (μg SbH_3 and AsH_3 min^{-1} vs charging time) were obtained from the amounts of SbH_3 and AsH_3 generated during various time intervals. The total hydride was obtained by summing the amounts from all the samples.

Data on current, voltage, ampere-hours, watt-hours, electrolyte temperature and charging time were stored on magnetic tape for later use. Ambient temperature was determined using a calibrated mercury-in-glass thermometer placed in the fume hood. Cell resistance was monitored during discharge by using a modification of the 'power ramp' method, 12 15-s current pulses, ranging from 25 to 1000 A (increasing in steps of $\sqrt{2}$) were drawn (with small capacity replacements) at discharges of 5, 50, 75 and 90% of the rated capacity. The cell current and voltage were monitored at each power ramp. The data were analyzed using the method of least squares, and values of cell resistance were calculated from the resulting equation. Internal resistance of the lead–acid cell were determined as a function of cell voltage during discharge.

2.4. *Chemical analysis*

The absorber solution reacts with SbH_3 and AsH_3 to produce Sb^{3+} and As^{3+} species. Antimony was determined by a spectrophotometric method [14] based on the measurement of the absorbance of SbI_4^-. Arsenic was determined by atomic absorption in an argon–hydrogen air-entrained flame, after reconversion to arsine. These methods provided adequate sensitivity for measuring the total generation of 25 μg SbH_3 and 1 μg AsH_3 (0.25 μg Sb and 0.01 μg As ml^{-1} of absorber solution). The coefficients of variation for the antimony and arsenic determinations in the optimum range were about 2 and 4%, respectively. Tests were conducted to assess the possibility of interference from H_2S, which could have been generated in the cell by reaction of hydrogen with the rubber lining of the cell separators. Mass spectral and gas chromatographic analysis showed the presence of little, if any, H_2S (detection limit was < 10 ppm) in the electrolysis gas. The possible interference from very small amounts of H_2S in the absorber solutions was also tested by measuring the arsenic content of several samples repeatedly over a 9-day period; no loss of arsenic by sulfide precipitation could be detected. Other tests showed that only insignificant amounts of arsine and stibine were lost during collection by decomposition and deposition on equipment walls.

3. Results

3.1. *Data collected*

The cell was operated for a total of 28 daily discharge/charge cycles, and 13 equalization charge cycles. The cell was discharged to 64, 72, 80 and 90% of the rated capacity. The resistance of the cell, measured as a function of per cent of the rated capacity discharged

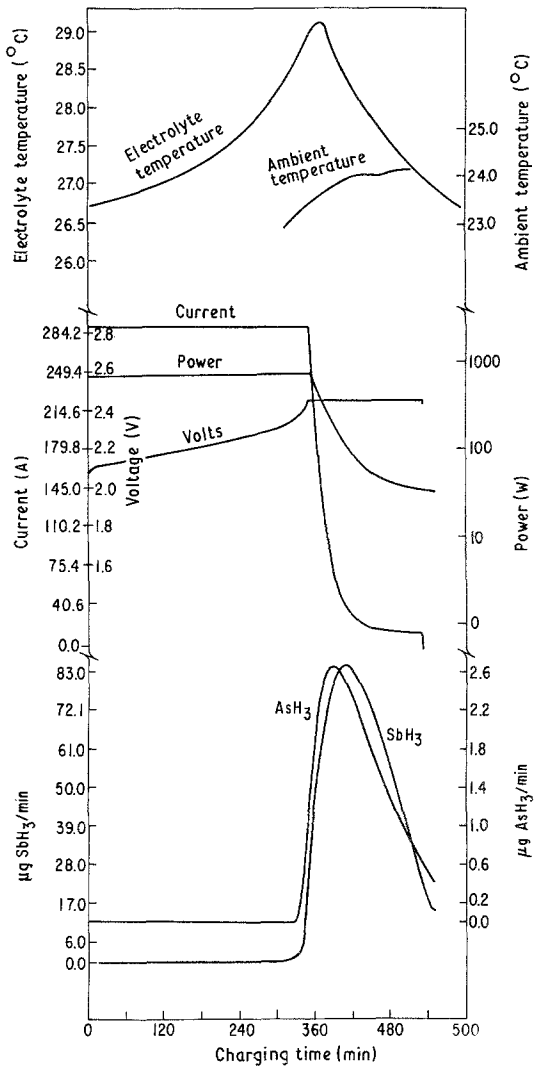

Fig. 5. Stibine and arsine generation rates, current, voltage, power and electrolyte temperature vs charging time for charge cycle C12.

(5, 50, 75 and 90%), as well as the concomitant changes in cell voltage, are plotted in Fig. 4. Cell electrical data, as well as ambient and electrolyte temperatures, are given in Table 1. The amounts of stibine and arsine generated by the cell during charge cycles of ~ 8 h and related weekly equalization charge cycles of 4 h are given in Table 2.

The experimental data obtained for successive daily equalization charge cycles at 2.55 and 2.45 V are given in Table 3. The amounts of antimony in the electrolyte before and after the equalization charge cycles were also determined and the results are included in Table 3.

3.2. *Effects of hydride generation on flow rate of nitrogen, depth of discharge of preceding cycles and peak electrolyte temperature*

Because the amounts of stibine and arsine collected during a charge cycle could depend on parameters such as flow rate of carrier gas through the cell, peak electrolyte temperature and capacity discharged during the preceding discharge cycle, even though the charging pattern may remain the same we measured the effect of these variables.

For the charge cycles C12, C16, C17, C18 and C20

Table 1. Electrical, electrolyte temperature and ambient temperature data

Cycle[a]		*Current (A)*			*Voltage (V)*			*A h*		*Ratio*[b] *charge (A h)/ discharge (A h)*		*Average ambient temp. (° C)*	*Peak electrolyte temp. (° C)*
No.	*Time (min)*	*Const.*	*Avg.*	*At end chg*	*Const.*	*Avg.*	*At end dischg*	*Chg*	*Dischg*	*I*	*II*		
C1	470		198.9			2.25		1510.0					
EC1	241		8.6		2.45			34.3					
D2	300	−290				1.98	1.89		−1450.4		1.06		
C2	460		194.5	12.6		2.26		1487.6					
D3	300	−290				1.97	1.89		−1450.8				
C3	464		194.3	13.5		2.26		1494.0				27.8	32.1
D4	300	−290				1.97	1.89		−1450.8	1.03			
C4	460		194.1	13.2		2.26		1494.2				26.3	31.7
D5	300	−290				1.96	1.89		−1451.0	1.03			
C5	463		194.3	12.2		2.26		1487.9				23.2	28.9
EC2	253		10.1	8.0	2.45			40.4				24.2	24.6
D6	300	−290				1.96	1.89		−1450.7		1.05		
C6	462		193.3	13.2		2.25		1488.7				25.6	31.0
D7	300	−290				1.96	1.89		−1450.7	1.03			
C7	469		193.7			2.27		1489.4				24.0	29.6
D8	300	−290				1.96	1.88		−1450.7	1.03			
C8	586		156.6	10.8		2.26		1511.4				23.2	28.9
D9	300	−290				1.96	1.88		−1450.6	1.04			
C9	587		156.3	5.0		2.26		1507.8				22.4	28.5
EC3	217		8.5	6.0	2.45			34.0				21.9	22.2
D10	300	−325				1.94	1.85		−1626.4	0.95			
C10	502		200.8	10.5		2.25		1653.6				22.3	28.0
D11	300	−360				1.92	1.81		−1801.6	0.92			
C11	538		206.0	13.0		2.24		1834.4				22.4	28.0
D12	300	−360				1.93	1.81		−1801.9				
C12	533		209.7			2.24		1839.2				23.5	29.1
D13	300	−360				1.92	1.81		−1801.8				
C13	532		210.1	13.8		2.24		1842.0				22.2	28.5
EC4	210		10.6	6.0	2.45			42.4				22.4	22.2
D14	300	−360				1.92	1.81		−1801.9	1.05			
C14	536		209.5	14.0		2.24		1852.8				23.0	29.5
D15	300	−360				1.92	1.81		−1801.9	1.03			
C15	519		212.0	14.0		2.24		1835.0				22.8	28.4
D16	300	−360				1.92	1.80		−1801.6	1.02			
C16	504		210.7	14.7		2.24		1843.3				21.9	29.1
D17	300	−360				1.92	1.81		−1801.9	1.02			
C17	520		211.6	15.7		2.24		1840.1					28.8
EC5	183		82.3		2.65			249.9				22.0	24.9
D18	300	−360					1.83		−1802.2		1.16		
C18	530		208.0	13.4		2.24		1844.0					28.6
D19	300	−405				1.90	1.74		−2027.5	0.91			
C19	518		216.8	14.7		2.23		2071.6				21.8	28.6
D20	300	−405				1.90	1.74		−2027.5	1.02			
C20	578		217.7	14.9				2075.6				22.1	28.8
D21	300	−405				1.90	1.72		−2027.5	1.02			
C21	580		219.3	16.3		2.22		2078.7				23.2	29.3
EC6	220			72.6	2.5							23.0	26.8
D22	300	−405					1.77		−2027.2				
C22	591		216.3	14.9				2093.7				24.1	31.6
D23	300	−405				1.91	1.77		−2072.2	1.03			
C23	587		216.6	15.6				2082.6				24.5	31.2
D24	300	−405				1.91	1.76		−2026.8	1.03			
C24	596			17.8		2.32		2148.2				26.1	31.1
EC7	194			32.0	2.55							24.3	27.1
C25													
C27													
EC8	208			27.5	2.55			114.9				22.6	

[a] C = charge, D = discharge and EC = equalization charge.

[b] SA h Chg (n) and SA h Dischg (n + 1) are the ampere-hours charged and discharged during the (n)th and (n + 1)th cycles, respectively; SA h Chg (4, 5) is total during cycles on Thursday and Friday; I = SA h Chg (n)/SA h Dischg (n + 1), I = SA h Chg (4, 5)/SA h Dischg [n(4, 5) + 1].

Table 2. Stibine and arsine generation during daily charge and weekly equalization charge cycles[a]

Cycle	Time (min)	Total hydride generation[b] (mg)			
		SbH_3	Average SbH_3	AsH_3	Average AsH_3
C2	460	13.8		0.40	
C3	464	13.4		0.46	
C4	460	12.6		0.42	
C5	463	10.7		0.32	
C6	462	12.0		0.35	
C7	469	11.4		0.35	
C8[c]	586	14.4		0.49	
C9[c]	588	13.0		0.34	
C10	502	9.8		0.25	
C11	538	10.0		0.31	
C12	533	11.8	12.1 ± 1.4	0.35	0.33 ± 0.06
C13	532	10.9		0.34	
C14	536	12.0		0.35	
C15	519	10.2		0.23	
C16	505	12.6		0.33	
C17	520	11.8		0.29	
C18	530	11.2		0.27	
C19	578	11.1		0.28	
C20	578	12.5		0.30	
C21	580	14.0		0.37	
C22	591	11.9		0.27	
C23	587	14.1		0.31	
C24	596	15.0		0.33	
EC1	240	7.4		0.12	
EC2	240	7.3	7.2 ± 0.4	0.15	0.11 ± 0.03
EC3	240	6.5		0.08	
EC4	240	7.4		0.18	
EC5	240	62.7	63.1 ± 0.5	0.32	0.33 ± 0.01
EC6	240	63.4		0.34	
EC7	240	26.0	25.5 ± 0.7	0.23	0.23 ± 0.01
EC8	240	25.0		0.22	

[a] Duration of charge cycles (C), ~8 h including 3 h of overcharge; duration of equalization charge cycles (EC), ~4 h.
[b] Stibine and arsine totals for EC cycles, each of 4-h duration, were obtained by an extrapolation procedure using a four-point least-square quadratic fit of experimental data points.
[c] Not included in averaging.
Equalization charge at (a) 2.45 V, (b) 2.65 V and (c) 2.55 V.

in which the peak electrolyte temperature was found to be constant (28.8 ± 0.3° C), the amount of SbH_3 generated was found to be independent of the rate of the carrier gas flow through the cell within the experimental accuracy.

Table 3. Total amounts of stibine and arsine generated during successive 4-h equalization charge cycles[a]

Cycle No.	Open-circuit period between two cycles (h)	Total hydride (mg)		Sb in electrolyte[b] ($\mu g\,ml^{-1}$)	
		SbH_3	AsH_3	Before eq. charge	After eq. charge
EC9	*17.2*	*31.3*	*0.34*	–	*1.7*
EC10	*20.4*	*17.8*	*0.18*	*2.3*	*1.6*
EC11	*17.8*	*10.9*	*0.13*	*2.3*	*1.4*
EC12	*19.0*	*13.5*	*0.17*	*2.5*	*1.6*
EC13	*58.0*	–	–	–	*0.83*
EC14	*20.0*	*2.6*	*0.09*	–	*0.88*

[a] *Charge voltage, 2.55 V except for EC14 (2.45 V).*
[b] *Determined colorimetrically.*

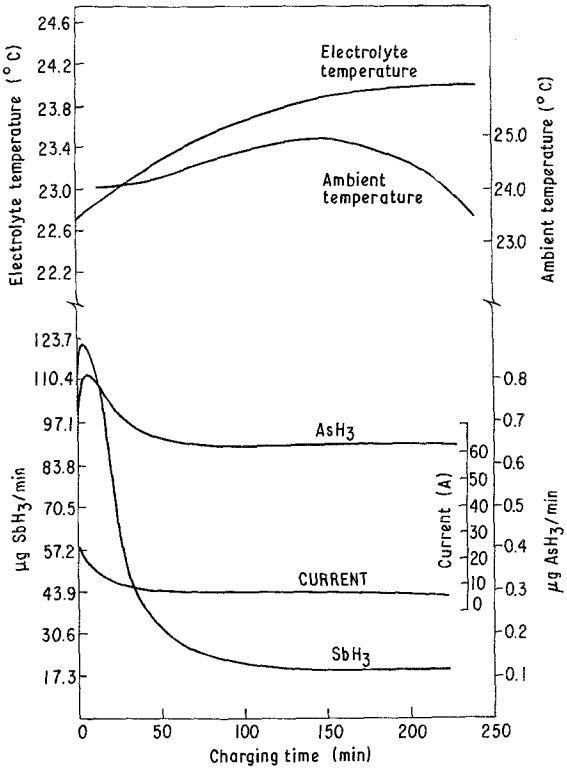

Fig. 6. Stibine and arsine generation rates, current, voltage, power and electrolyte temperature vs charging for equalization charge cycle EC2 at 2.45 V.

It was observed that variation of the extent of discharge, from 64 to 90% of rated capacity has little or no effect on the amount of SbH_3 generated during the charge cycle which follows.

The data suggest that the amount of SbH_3 generated in charge cycle of the lead–acid cell increases by approximately 0.7 mg per degree centigrade increase in the peak electrolyte temperature.

3.3. *Stibine and arsine generation rates and concomitant variation of electrical parameters during charge and equalization charge cycles*

The rates of stibine and arsine generation in $\mu g\,min^{-1}$, as a function of charging time, were computed and plotted for representative charge cycles and equalization charge cycles; a representative plot is shown in Fig. 5. The variations of cell parameters as a function of charging time are also shown in the figures. The variations of stibine and arsine generation rates, as well as of current, with charging time during equalization charge cycles at 2.65, 2.55 and 2.45 V are given in Figs 6–8 for comparison.

3.4. *Effect of equalization charge voltage on stibine and arsine generation*

As expected, the quantity of SbH_3 and AsH_3 generated during an equalization charge cycle is a strong function of the cell voltage. This variation is illustrated in Figs 6–8 and Tables 1 and 2.

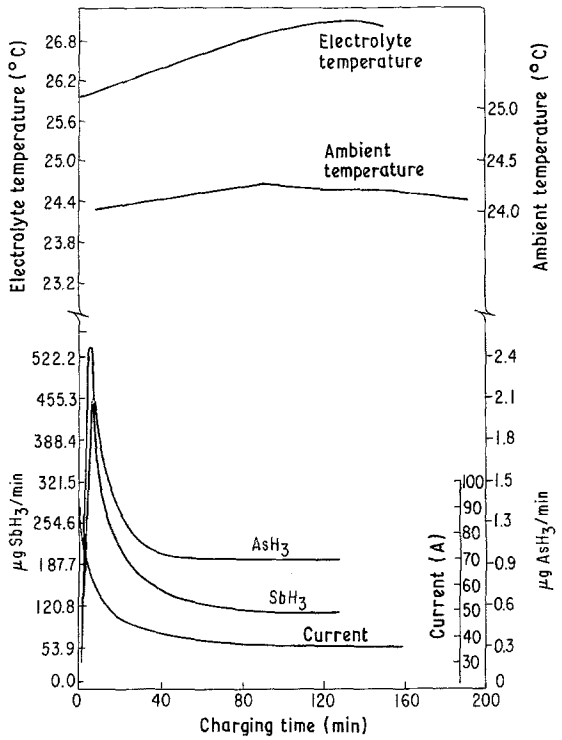

Fig. 7. Stibine and arsine generation rates, current, voltage, power and electrolyte temperature vs charging time for equalization charge cycle EC7 at 2.55 V.

3.5. *Stibine and arsine generation during successive daily equalization charging*

The stibine and arsine generated during successive daily equalization charges at 2.55 V were collected at various times during each equalization charge cycle and analyzed. The total emission of the toxic hydrides, as well as the stibine and arsine generation profile, was obtained for each cycle. The cell was kept on open circuit between the end of an equalization charge cycle and the beginning of the next equalization charge. The antimony content of the electrolyte near the cell top was determined before and after each equalization charge cycle. The experimental data are given in Table 3 and are graphically presented in Fig. 9.

4. Discussion

The modes of charging of lead–acid cells in the studies [6, 7] of stibine generation reported in the past bear little resemblance to the contemplated utility load-leveling duty cycle. Hence data obtained in these studies cannot be used to estimate concentration levels of the stibine in the contemplated load-leveling lead–acid battery facilities. Furthermore, no quantitative investigation of arsine generation during the charging of a state of the art lead–acid cell has ever been reported.

The present study, for the first time, provides quantitative data on the total emission of stibine and arsine and the rates of generation of these gases during charge and equalization charge cycles. The results obtained suggest a correlation between the rates of generation of the toxic hydrides and the charging parameters. The rates of generation of stibine and arsine during typical charge cycles take a steep climb

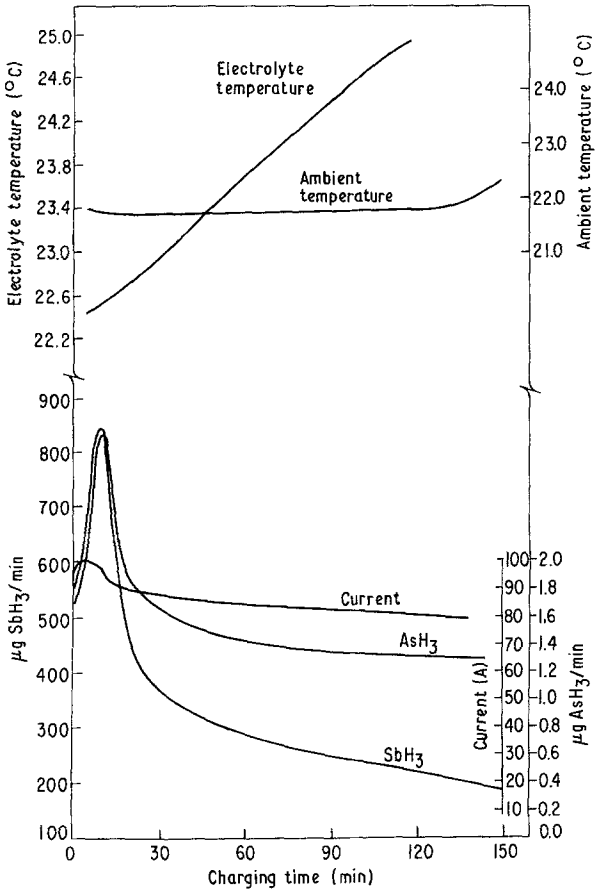

Fig. 8. Stibine and arsine generation rates, current, voltage, power and electrolyte temperature vs charging time for equalization charge cycle EC5 at 2.65 V.

at the threshold cell voltage of 2.40 V. The high rates of stibine and arsine generation usually persist over the initial 1.5–2.0 h of the overcharge period. The rate levels off after 2.5 h. Only a minute fraction continues to be carried out of the cell by the carrier gas stream during the open-circuit period immediately following the charge cycle. The rates of hydride generation were very high for the first 20 min of the initial portion of an equalization charge cycle and leveled off to almost uniform rates soon thereafter. The rates are strong functions of cell voltage, the maximum being observed at 2.65 V. A summary of the stibine and arsine emissions from the experimental lead–acid cell in a typical charge and equalization charge cycle is given in Table 4. The numbers in this

Table 4. Stibine and arsine generation from lead–acid cell

Experiments	*Total generation (mg)*	
	SbH_3	AsH_3
Charge cycle[a]	12.1 ± 1.4	0.33 ± 0.06
Equalization[b]		
2.45 V	7.2 ± 0.4	0.11 ± 0.03
2.55 V	25.5 ± 0.7	0.23 ± 0.01
2.65 V	63.1 ± 0.5	0.33 ± 0.01

[a] 23 cycles, 8 h cycle includes 3 h of overcharge.
[b] 4 cycles, 2.45 V, 4 h each; 2 cycles, 2.55 V, 4 h each; 2 cycles, 2.65 V, 4 h each.

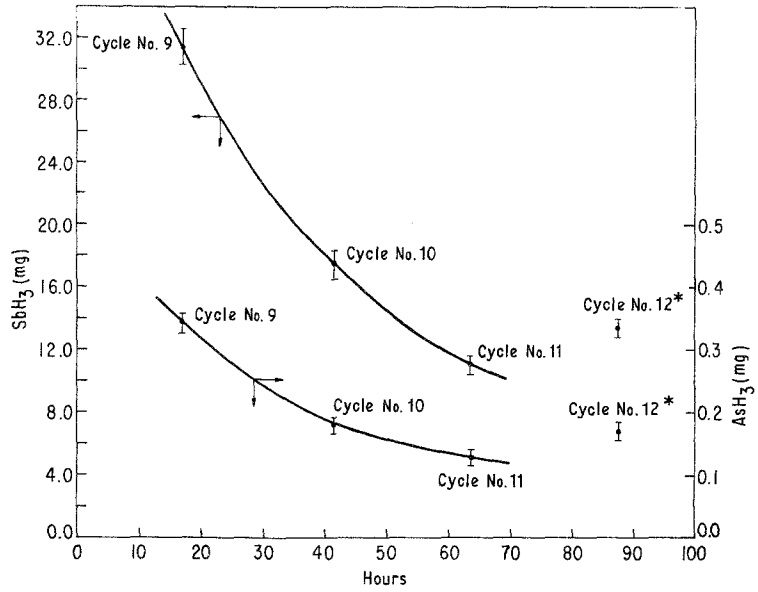

Fig. 9. Total stibine and arsine generated in successive equalization charging at 2.55 V. *Higher antimony concentration in the electrolyte before start of the charge cycle.

table were derived by averaging all the applicable data from our experimental results.

The data in Table 3 indicate that the total weight of SbH_3 and AsH_3 generated decreases rapidly during successive charge cycles, with very little being generated during the sixth charge cycle. The amount of SbH_3 continues to be higher than the AsH_3, probably because there is more antimony in the current collector grid.

A number of previous studies [13, 14] were directed towards understanding the mechanism and factors controlling the generation of stibine. Antimony originally contained in the positive and negative grids was found, after a number of discharge/charge cycles, to be distributed in the active material of the positive plate, the electrolyte, the active metal of the negative plate and the gaseous stibine produced at the negative electrode.

The corrosion of antimony in the positive electrode, its transport toward the negative electrode and its deposition on the negative electrode undoubtedly play significant roles in determining the rate of stibine generation. The stibine generation rate depends on a number of competing processes, namely the rate of leaching of antimony from the grids (in particular, the positive grid) into the electrolyte, transport of antimony species towards the negative plate and electrodeposition of antimony on the negative plate. A possible explanation for the observed decline in stibine generation during successive equalization charges is the depletion and inadequate replenishment of freshly deposited antimony on the negative plate. This is clearly shown in our measurements of antimony in the electrolyte (see Table 3). A slight reversal of this trend, which was observed in cycle EC12 (see Table 3), may have been due to the higher concentration of antimony in the electrolyte before initiation of that charge cycle, as indicated in Table 3. The maxima in the rate profiles for stibine generation for all the charge cycles may also be explained by this depletion of freshly electrodeposited antimony, which is in limited supply. Further experimental work is required to obtain a definitive understanding of the mechanisms of the chemical and electrochemical effects governing both stibine and arsine generation in lead–acid cells.

5. Conclusions

This study has demonstrated the applicability of analytical methods for the determination of SbH_3 and AsH_3 in battery off-gases and has provided quantitative data that are useful for estimating stibine and arsine generation during normal operation of a state of the art industrial lead–acid battery in a load-leveling duty cycle.

The rate profiles for stibine and arsine generation from lead–acid batteries may be reduced to insignificant amounts if the voltages during charge cycles and equalization charge cycles in any weekly discharge/charge schedule are kept at or below 2.40 V. However, such a charging procedure may not be acceptable in utility load-leveling application, because it may lead to a continuous decline in cell capacity.

Acknowledgements

The authors wish to express their thanks to P. T. Cunningham, K. J. Jensen, A. G. Engelkemeir, A. M. Essling, I. M. Fox, M. I. Homa, W. E. Streets, R. J. Meyer and F. L. Williams for their efforts in analyzing the samples and to L. E. Ross, J. L. Settle, R. W. Kessie and R. C. Elliott for technical assistance during the course of the testing program. The authors also express their thanks to C & D Batteries for supplying the lead–acid cell for the experiments. The work was supported by the Energy Storage Division, US Department of Energy, under Contract W-31-109-Eng-38.

References

[1] N. I. Sax, 'Dangerous Properties of Industrial Material', 6th Edn, Van Nostrand Reinhold, New York (1984) pp. 323, 2465.

[2] S. F. Dudley, *J. Ind. Hyg.* **1** (1919) 215.
[3] H. Halasko and M. Maslowski, *Reczniki Chem.* **10** (1930) 240.
[4] H. W. Salzberg and A. J. Andreatch, *J. Electrochem. Soc.* **101** (1954) 528.
[5] L. Tomilson, *J. Electrochem. Soc.* **111**, (1964) 592.
[6] H. E. Haring and K. G. Compton, *Trans. Electrochem. Soc.* **68** (1935) 283.
[7] R. Holland, 'Proc. Int. Symp. Batteries', Christ Church, Hants, England (October 1958) p. 21.
[8] A. B. Ashendorf and H. P. Murphy, 'Summary Report on Stibine and Arsine', Electric Storage Batteries Inc., Report of 8 May (1951).
[9] B. H. Schubert and C. S. Parker, 'The Effect of Lead–Antimony Grid Alloys on the Storage Battery Behaviour', National Battery Manufacturers Meeting, White Sulfur Springs, W. Virginia, 11–18 May (1939).
[10] I. A. Aguf, M. A. Dasoyan, A. I. Rusin and A. P. Batin, *Electrotekhnika* **3** (1972) 61; *Sbornik Rabot Po Khimiches Kim Toka Nauchno-Issledpvatelskil Akkumulyatorniyi Inst.* **6** (971) 10.
[11] W. Herrman and G. Proposti, *Z. Electrochemie* **61** (1957) 1154; W. Herman, W. Ilge and G. Proposti, 'Proc. 2nd Int. Conference on Peaceful Uses of Atomic Energy', 1958, Pergamon Press, Oxford (1959).
[12] H. Leibssle and E. Zehender, *Bosch Techn. Berichte* **3** (1970) 163.
[13] R. Varma, Z. Tomczuk and N. P. Yao, presented at the Utility Load-Leveling Symposium, 152nd Electrochem. Soc. Meeting, Atlanta, GA, 10–14 October (1977), 'Extended Abstracts', Vol. 77, (1977) p. 391; R. Varma, G. M. Cook and N. P. Yao, 'Proc. of the Second U.S. DOE Environmental Control Symposium', Reston, VA, 17–19 March (1980); U.S. DOE Report No. Conf. 800334/2, (1980) 709.
[14] R. Holland, *Analyst* **87**(1962) 385.